Long-chain acyl-CoA synthetases activate fatty acids for lipid synthesis, remodeling and energy production in Chlamydomonas

Fan Bai, Lihua Yu, Jianan Shi, Y. Li-Beisson, Jin Liu

New Phytologist

Long-chain acyl-CoA synthetases activate fatty acids for lipid synthesis, remodeling and energy production in Chlamydomonas

Journal:	*New Phytologist*
Manuscript ID	NPH-MS-2021-37386
Manuscript Type:	MS - Regular Manuscript
Date Submitted by the Author:	28-Jul-2021
Complete List of Authors:	Bai, Fan ; Peking University, College of Engineering Yu, Lihua; Peking University, College of Engineering Shi, Jianan; Peking University, College of Engineering Li-Beisson, Yonghua; CEA, Department of Plant Biology Liu, Jin; Peking University, College of Engineering
Key Words:	Acyl activation, fatty acid β-oxidation, lipid droplet, lipid homeostasis, lipid remodeling, N recovery, triacylglycerol

Long-chain acyl-CoA synthetases activate fatty acids for lipid synthesis, remodeling and energy production in Chlamydomonas

Fan Bai[1], Lihua Yu[1], Jianan Shi[1], Yonghua Li-Beisson[2], Jin Liu[1,*]

[1]Laboratory for Algae Biotechnology and Innovation, College of Engineering, Peking University, Beijing 100871, China

[2]Aix Marseille Univ, CEA, CNRS, BIAM, Institut de Biosciences et Biotechnologies Aix-Marseille, CEA Cadarache, Saint Paul-Lez-Durance 13108, France

[*]Corresponding author: Jin Liu (gjinliu@pku.edu.cn)

Running title: Roles of LACS members in algal lipid homeostasis

Word count

Main body: 6387; Introduction: 980; Materials and Methods: 1149; Results: 2313; Discussion: 1945.

Figures: 8; **Tables**: 0; **Supporting information**: 12 supplementary figures, 1 supplementary table, and 2 data sets.

Summary

- Long-chain acyl-CoA synthetases (LACSs) play many roles in mammals, yeasts and plants, but knowledge on their functions in microalgae remains fragmented. Here via genetic, biochemical and physiological analyses, we unraveled the function and roles of LACSs in the model microalga *Chlamydomonas reinhardtii*.
- *In vitro* enzymatic activity assays on purified recombinant proteins revealed that CrLACS1, CrLACS2 and CrLACS3 all exhibited bona fide LACS activities toward a broad range of free fatty acids.
- The Chlamydomonas mutants compromised in CrLACS1, CrLACS2 or CrLACS3 didn't show obvious phenotypes in lipid content or growth under nitrogen (N)-replete condition. But under N-deprivation, *CrLACS1* or *CrLACS*2 suppression resulted in ~50% less oil, yet with a higher amount of chloroplast lipids. By contrast, *CrLACS3* suppression impaired oil remobilization and cell growth severely during N-recovery, supporting its role in fatty acid β-oxidation to provide energy and carbon sources for regrowth. Transcriptomics analysis suggested that the observed lipid phenotypes are likely not due to transcriptional reprogramming but rather a shift in metabolic adjustment.
- Taken together, this study provided solid experimental evidence for essential roles of the three Chlamydomonas LACS enzymes in lipid synthesis, remodeling and catabolism, and highlighted the importance of lipid homeostasis in cell growth under nutrient fluctuations.

Keywords

Acyl activation, fatty acid β-oxidation, lipid droplet, lipid homeostasis, lipid remodeling, N recovery, triacylglycerol

Introduction

Microalgae have emerged as a promising platform for production of food, fuels and synthons for green chemistry (Tang *et al.*, 2016; Levasseur *et al.*, 2020). Many of the potential applications are related to their capacity in synthesizing and accumulating a wide range of fatty acid structures and the potential for high amount of neutral lipids e.g. triacylglycerol (TAG) or oil (Hu *et al.*, 2008). Fatty acids are building blocks of membrane and storage lipids and serve as important substrates for carbon and energy storage, energy production, acylation of proteins and for lipid-based signaling (Glatz & Luiken, 2015; Resh, 2016; De Carvalho & Caramujo, 2018). To fulfil above functions, fatty acids need to be activated either to acyl carrier proteins (ACPs) in the chloroplast or to Coenzyme A (CoA) in the extra-chloroplast compartments and the latter process is mediated by the ATP-dependent long-chain acyl-CoA synthetases (LACSs) (Li-Beisson *et al.*, 2015; Zhao *et al.*, 2021). Acyl-CoAs are important metabolic intermediates in *de novo* acyl-lipid synthesis, in re-integration of free fatty acids (FFAs) coming from membrane lipid degradation back to lipid metabolism and in mediating fatty acid β-oxidation in peroxisomes, among others. Therefore, LACS enzymes play a central role in acyl-lipid metabolism.

The functions and physiological roles of LACS family have been well studied in many organisms including bacteria, yeasts, vascular plants and mammals (DiRusso & Black, 1999; Coleman *et al.*, 2002; Shockey *et al.*, 2002; Zhao *et al.*, 2010; Watkins & Ellis, 2012; Zhao *et al.*, 2019; Ayaz *et al.*, 2021) but rare in microalgae. For example, *Escherichia coli* harbors a single LACS encoded by the *FadD* gene, which resides at the inner membrane of cell envelope and converts FFAs to acyl-CoAs for downstream lipid metabolism (Black *et al.*, 1992). It also functions in combination with the outer membrane-bound fatty acid transport protein FadL to facilitate import of exogenous FFAs (DiRusso & Black, 1999). On the other hand, there are four LACS isoforms reported in *Saccharomyces cerevisiae*, namely, Faa1p through Faa4p (Johnson *et al.*, 1994; Knoll *et al.*, 1995). Whilst Faa1p, Faa3p and Faa4p are involved in activation of FFAs to form acyl-CoAs for lipid synthesis (Færgeman *et al.*, 2001; Kamisaka *et al.*,

2007), Faa2p functions in peroxisomes for fatty acid β-oxidation (Hettema *et al.*, 1996). Moreover, Faa1p or Faa4p cooperates with a plasma membrane-bound fatty acid transporter, Fat1p, to facilitate import of exogenous FFAs (Zou *et al.*, 2003).

By contrast, there are many more LACS isoforms in vascular plants, e.g., nine in Arabidopsis (Shockey *et al.*, 2002) and they are present in plastid, ER or peroxisomes (Schnurr *et al.*, 2002; Fulda *et al.*, 2004; Zhao *et al.*, 2010). Despite all nine LACS isoforms (LACS1 through LACS9) function in converting FFAs to acyl-CoAs *in vitro* (Shockey *et al.*, 2002), their roles in Arabidopsis are multifaceted (Fulda *et al.*, 2002; Schnurr *et al.*, 2002; Fulda *et al.*, 2004; Lü *et al.*, 2009; Weng *et al.*, 2010; Zhao *et al.*, 2010; Jessen *et al.*, 2011; Jessen *et al.*, 2015; Zhao *et al.*, 2019). It has been demonstrated that the three ER LACS (LACS1, LACS2 and LACS4) are involved in cuticular lipid metabolism in Arabidopsis (Lü *et al.*, 2009; Weng *et al.*, 2010; Jessen *et al.*, 2011). The peroxisomal LACS6 and LACS7, on the other hand, have overlapping roles in fatty acid β-oxidation and are essential for seedling development (Fulda *et al.*, 2002; Fulda *et al.*, 2004). Albeit being of close phylogenetic relationship, LACS8 and LACS9 are targeted to the ER and plastid outer envelope, respectively (Schnurr *et al.*, 2002; Zhao *et al.*, 2010). Interestingly, LACS9, but not LACS8, functionally overlaps with LACS1 in seed TAG biosynthesis (Zhao *et al.*, 2010). Moreover, both LACS8 and LACS9 have functional overlap with LACS4 in TAG synthesis in seeds (Jessen *et al.*, 2015; Zhao *et al.*, 2019). In this context, there is a complex network of functions and interactions among LACS isoforms in Arabidopsis (Zhao *et al.*, 2019).

Only limited efforts have so far been made on studying LACSs from microalgae and their functional roles *in vivo* remain largely unknown (Zhang *et al.*, 2012; Guo *et al.*, 2014; Jia *et al.*, 2016; Li *et al.*, 2016; Wu *et al.*, 2020). The green alga *Chlamydomonas reinhardtii* (hereafter Chlamydomonas) has been widely used as a unicellular model autotroph for studying lipid metabolism (Merchant *et al.*, 2012; Li-Beisson *et al.*, 2015; Kong *et al.*, 2019). There are three putative LACS-coding genes in Chlamydomonas genome, namely, *CrLACS1*, *CrLACS2* and *CrLACS3* (Li-Beisson *et al.*, 2015). It has been reported that suppression of *CrLACS2* by insertional

mutagenesis impaired TAG accumulation under nitrogen (N)-deprivation (Li *et al.*, 2016). Knockdown of *CrLACS1* or *CrLACS3* via RNA interference was reported to result in free fatty acid secretion (Jia *et al.*, 2016). Nevertheless, evidence is still lacking with respect to how they function in lipid metabolism and their respective roles in lipid homeostasis during Chlamydomonas' response to nutrient fluctuations.

In the present study, to reveal the function and physiological roles of CrLACS members in Chlamydomonas, we conducted a multifaceted study by systematically integrating *in vitro* LACS enzymatic activity assays, growth and lipidomic analyses of insertional mutants and their corresponding complemented strains, and comparative transcriptomics. All three LACSs were demonstrated as bona fide LACS enzymes and showed activities toward a broad range of FFAs without apparent substrate preference. Both CrLACS1 and CrLACS2 were involved in N-deprivation induced TAG synthesis, with the former being more transcriptionally stimulated and likely playing a more important role in TAG accumulation than the latter. Furthermore, CrLACS1 and CrLACS2 were found to participate in directing acyl flux to TAG or chloroplast membrane lipids. CrLACS3, on the other hand, was involved in TAG catabolism under N-recovery to provide carbon precursors and energy for cell growth via the fatty acid β-oxidation. We also discussed the possible spatial and temporal coordination of the three CrLACS isoforms in maintaining lipid homeostasis in Chlamydomonas in response to nutrient fluctuations.

Materials and Methods

Algal strains and culture conditions

The Chlamydomonas wild-type (WT) CC-5325 and insertional mutants including *crlacs1-1* (LMJ.RY0402.173140), *crlacs1-2* (LMJ.RY0402.129310), *crlacs2-1* (LMJ.SG0182.015843), and *crlacs3-1* (LMJ.RY0402.199483) were purchased from the Chlamydomonas Resource Center. All strains were cultivated in Tris-Acetate-Phosphate (TAP) medium under continuous illumination of 50 μmol m^{-2} s^{-1} and 150 rpm shaking at 23˚C. For N-replete growth, cells were inoculated in TAP medium at a

cell density of 1×10^6 cells mL^{-1} and allowed to grow for 3 days. The algal cells were then harvested by centrifuging, washed twice with N-free TAP medium (TAP-N) and finally re-suspended in TAP-N at a cell density of 3×10^6 cells mL^{-1} for N-deprivation treatment (ND). After 3 days of ND, cells were collected and equal volumes of TAP-N were replaced by Tris-Minimal Medium (MM), followed by 3 days of growth in the dark for N-recovery treatment (NDR).

Cell number and dry weight measurements were performed according to our previously described procedures (Liu *et al.*, 2016a). For visualization of lipid droplets (LDs), cells were stained with the fluorescent dye BODIPY 505/515 (Molecular Probes, OR, USA) at a final concentration of 1 μg mL^{-1} for 10 min at room temperature, and then observed under an Olympus BX51 fluorescence microscope (Olympus, Japan).

RNA isolation and RT-qPCR

Total RNA was isolated from algal samples (ca. 10^7 cells) using TRI reagent (Invitrogen, Carlsbad, CA) according to the manufacturer's instructions. The cDNA synthesis and RT-qPCR were performed following our previously described procedures (Liu *et al.*, 2016a). Primers used for RT-qPCR are listed in Table S1. The gene expression levels were expressed relative to the internal control β-actin gene.

Functional assessment of CrLACS1, CrLACS2 and CrLACS3 in yeast

The coding sequences of *CrLACS*s were PCR amplified using primers listed in Table S1 and sub-cloned into the yeast expression vector pYES2-CT (Invitrogen). The resultant plasmids (Fig. S1a) were each transformed into the *S. cerevisiae* strain YB525 using S.c. EasyComp Transformation Kit (Invitrogen). YB525 is defective in the LACS-coding genes *Faa1* and *Faa4* and thus cannot grow on FFAs as the sole carbon source (Zou *et al.*, 2003). For growth test, YB525 cells expressing *CrLACS* genes were first cultured in yeast synthetic medium lacking uracil (SD/-ura) containing 2% (w/v) galactose for 4 h to induce *LACS* expression, followed by removal of galactose and supplementation with FFAs at a concentration of 100 μM and incubation at 30˚C for

ten days (Wu *et al.*, 2020). The FFA stock solutions were prepared in 10% isopropanol containing 1% Triton-100. Yeast cell densities were recorded as OD_{600}.

Purification of recombinant CrLACS1, CrLACS2 and CrLACS3 and *in vitro* enzymatic activity assay

The coding sequences of *CrLACS* genes were PCR amplified using primers listed in Table S1 and sub-cloned into the *E. coli* expression vector pET32a. The resultant plasmids (Fig. S1b) were each transformed into the *E. coli* strain BL21 (DE3), using pET32a as the control. To induce protein expression, *E. coli* cells carrying *CrLACS* genes were grown at 16˚C for 16 h in the presence of 1 mM isopropyl-β-thiogalactoside (IPTG). Then, *E. coli* samples were collected and lysed by sonication, followed by centrifugation at 13,000 *g* for 15 min to remove cellular debris. The supernatant was loaded onto a prepacked HisPur Ni-NTA column (ThermoFisher Scientific, Waltham, MA, USA). To elute the target protein off the column, elution buffer that contains 200 mM imidazole, 500 mM NaCl, and 20 mM Tris-HCl buffer (pH 8.0) was applied and the effluent was dialyzed against 100 mM Tris-HCl buffer (pH 8.0) to remove imidazole. A 30 kDa cut-off concentrator (Millipore, Billerica, MA, USA) was used to concentrate the target protein. The purified protein was subjected to SDS-PAGE analysis. The *in vitro* activities of CrLACS isoforms were measured using an enzyme-coupled method (Ichihara & Shibasaki, 1991) with a few modifications (Wu *et al.*, 2020). LACS enzymatic activities were expressed as nmol acyl-CoA synthesized per min per mg protein.

Molecular characterization of insertional mutants of CrLACS1 and CrLACS3

The mutants were streaked on TAP agar plates for colony formation. A single colony from each mutant was then picked up and allowed to grow in liquid medium for reproduction. To confirm the insertions, three PCR reactions using genomic DNA as a template were conducted for each mutant, following the ChlaMmeSeq protocol (Zhang *et al.*, 2014), which were (1) the predicted insertion site using the suggested primer pair

(https://www.chlamylibrary.org), (2) the 5' end of insertion cassette-genome junction, and (3) the 3' end of insertion cassette-genome junction. Moreover, RT-qPCR was employed to check the effect of insertions on transcriptional expression of *CrLACS* genes. The primers were listed in Table S1.

Functional complementation of mutants defected in CrLACS1 or CrLACS3

The coding sequences of *CrLACS1* and *CrLACS2* were each sub-cloned into the Chlamydomonas expression vector pOpt_Clover_Hyg (Lauersen *et al.*, 2015). The resultant plasmids (Fig. S1c) were introduced into *crlacs1-1* and *crlacs3-1*, respectively, for functional complementation, using the glass bead-mediated transformation method (Kindle, 1990). The transformed cells, after overnight recovery under dim light, were selected on TAP medium supplemented with 15 μg mL^{-1} hygromycin under continuous illumination of 50 μmol m^{-2} s^{-1}. Putative colonies were verified by genomic PCR and RT-qPCR.

Lipid extraction and analysis

Lipids from yeast or Chlamydomonas were extracted with chloroform–methanol (2:1, v/v) as previously described (Liu *et al.*, 2016a). To separate lipids by thin-layer chromatography (TLC), lipids were loaded on silica gel 60 TLC plates (Merck, Germany) and developed with a mixture of hexane/tert-butylmethyl ether/acetic acid (80/20/2, by vol) for neutral lipids and with a mixture of chloroform/methanol/acetic acid/water (25/4/0.7/0.3, by vol) for polar lipids (Liu *et al.*, 2016b). Individual lipids on TLC plates were then stained with iodine vapor and recovered for subsequent transesterification experiments.

Total lipids and recovered fractions of individual lipid classes were transesterified to fatty acid methyl esters and then analyzed using an Agilent 7890 capillary gas chromatograph equipped with a 5975C mass spectrometry detector and a HP-88 capillary column (60 m×0.25 mm) (Agilent Technologies, Santa Clara, CA), and quantified according to our previously described procedures (Liu *et al.*, 2019).

RNA sequencing and differentially expressed gene analysis

WT, *crlacs1-1*, *crlacs2-1* and *crlacs3-1* under ND and NDR conditions were sampled (biological duplicates) for RNA extraction. After treatment with RNase-free DNase I (TaKaRa, Japan), total RNA (ca. 10 μg) from each sample was used for transcriptome library construction and sequencing as detailed in our previous study (Shi *et al.*, 2020). The clean reads were aligned to the genome of *C. reinhardtii* v5.5 in Phytozome v.12 (https://genome.jgi.doe.gov/portal/pages/dynamicOrganismDownload.jsf?organism=Phytozome) with the software TopHat (version 2.0.4) (Trapnell et al., 2012). Reads mapping to more than one location were excluded. The transcriptome data were submitted to the NCBI SRA database with the accession number PRJNA736801. The gene transcriptional abundance was expressed as fragments per kilobase million (FPKM). Differentially expressed genes (DEGs) between mutants and WT met the following requirements: at least a 2-fold change with Padjust < 0.001 and the FPKM value of either sample > 1.

Results

Chlamydomonas encodes three putative LACSs with distinct subcellular locations

Chlamydomonas harbors three putative LACS isoforms, CrLACS1, CrLACS2 and CrLACS3. To understand the evolution of CrLACSs, a phylogenetic tree was constructed using the three LACS proteins and the homologs from other organisms (Fig. S2). Apparently, CrLACS1 and CrLACS2 are closely related to *Chromochloris zofingiensis* LACS2-4 and clustered with Arabidopsis LACS1, LACS4 and LACS5, which are ER-localized (Zhao *et al.*, 2019; Wu *et al.*, 2020). Interestingly, proteomics analysis of purified lipid droplets (LDs) revealed association of CrLACS2 (Moellering & Benning, 2010; Nguyen *et al.*, 2011) and the *C. zofingiensis* CzLACS2-4 (Wang *et al.*, 2019) to LDs. This is reasonable as cytosolic LDs are believed to be derived from the ER (Ischebeck *et al.*, 2020) and thus may contain ER proteins including LACSs. Taken together, CrLACS1 and 2 are likely ER proteins and with CrLACS2 being

enriched in LD fraction.

CrLACS3, on the other hand, is closely related to *C. zofingiensis* LACS5 and clustered with Arabidopsis LACS6 and LACS7, known to be peroxisome-localized (Fulda *et al.*, 2004; Wu *et al.*, 2020). This, together with the fact that the Chlamydomonas fatty acid β-oxidation occurs in peroxisomes (Kong *et al.*, 2017), makes it highly likely that CrLACS3 is located in peroxisomes where it activates free fatty acids for β-oxidation.

Dynamic growth, TAG levels and transcriptional expression of *CrLACS* genes in Chlamydomonas in response to changing N status

N-deprivation is one of the most well studied stimuli for inducing TAG synthesis in algae (Valledor *et al.*, 2014; Park *et al.*, 2015; Liu *et al.*, 2016a; Liu *et al.*, 2019). To understand the role of CrLACS members in cell growth and TAG metabolism, Chlamydomonas cells were first cultured in TAP medium (N-replete or NR condition), then in N-free TAP medium (N-deprivation or ND condition) to induce TAG synthesis and finally in the minimal medium (with N but without acetate) in the dark (N-recovery or NDR condition) for TAG remobilization (Fig. 1a). Chlamydomonas grew fast during NR, followed by severely impaired growth during ND and rapid regrowth during NDR (Fig. 1b). Total fatty acid (TFA) content rose upon ND and reached a 2.8-fold increase after 3 days, suggesting active *de novo* fatty acid synthesis. A decline in TFAs during NDR was observed, indicating the occurrence of fatty acid catabolism (Fig. 1c). Similarly, TAG content increased upon ND yet to a much greater extent (21.2-fold) and then declined under NDR (Fig. 1c). The NDR-associated TAG decline is attributed to TAG catabolism.

Upon ND, *CrLACS1* exhibited a considerable up-regulation and its transcript level at 72 h reached 4.9-fold greater than that at 0 h; in response to NDR treatment, *CrLACS1* was dramatically down-regulated within 12 h (Fig. 1d). Similar to *CrLACS1*, *CrLACS2* was up-regulated by ND and showed a rapid down-regulation within 12 h of NDR (Fig. 1d). *CrLACS3*, differing from *CrLACS1* and *CrLACS2*, had slight transcriptional

changes during the ND period; upon NDR after 12 h, *CrLACS3* was up-regulated substantially (Fig. 1d). Taken together, the dynamics of TAG content and *CrLACS*s' transcriptional expression pattern suggest that CrLACS1 and CrLACS2 are likely involved in TAG biosynthesis while CrLACS3 in TAG catabolism. Interestingly, *CrLACS1* and *CrLACS2* also exhibited a transcriptional up-regulation after 12 h of NDR (Fig. 1d). Probably, cell regrowth begins after 12 h of NDR and needs regeneration of enough membrane lipids, in which *CrLACS1* and *CrLACS2* are required.

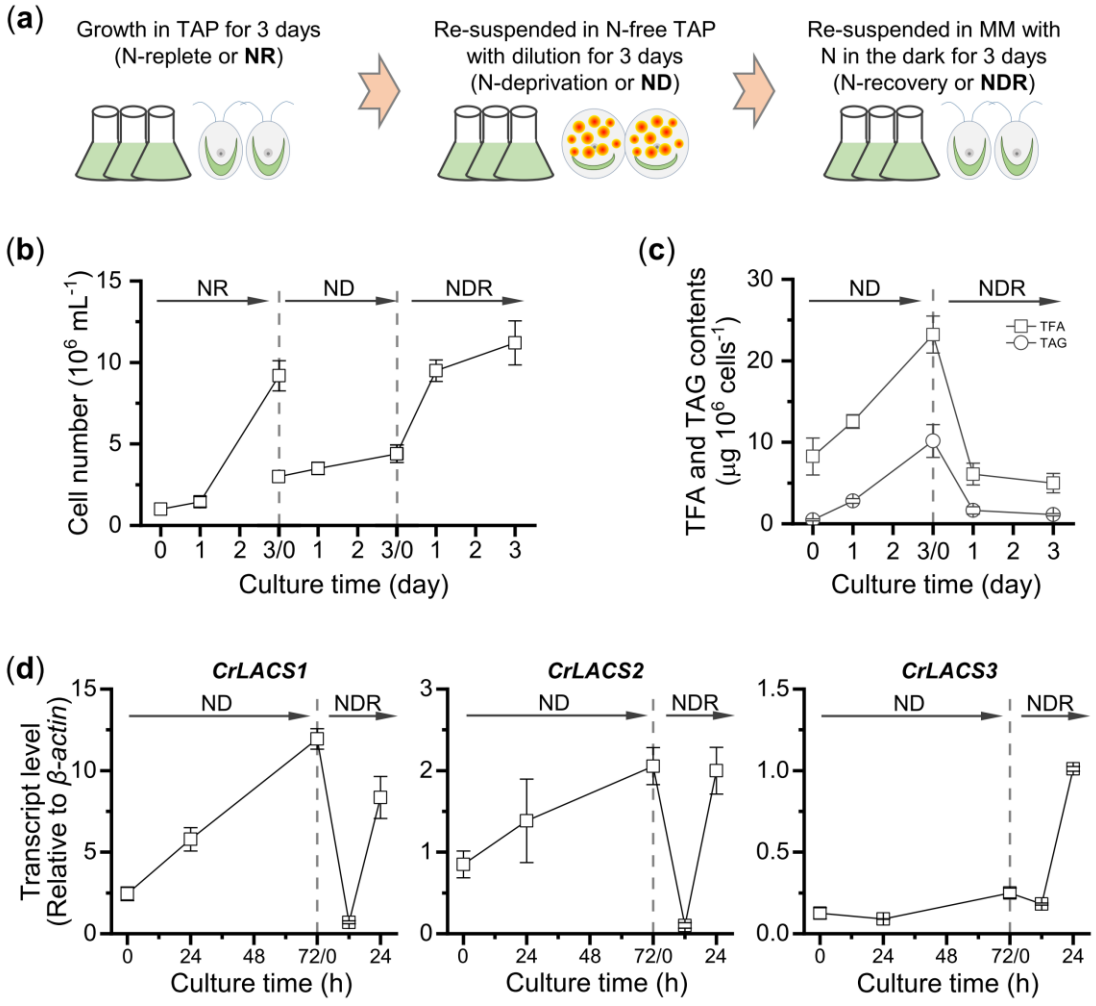

Fig. 1 Growth, lipid levels and transcriptional expression of *CrLACS* genes in Chlamydomonas under various N status. (a) Schematic illustration of three-stage culture conditions (sequentially N replete - NR, N deprivation - ND, then N deprivation-then-recovery - NDR). (b) Cell numbers. (c) TFA and TAG contents. (d) Transcript levels of *CrLACS1*, *CrLACS2* and *CrLACS3* relative to the internal control gene *β-actin*, quantified by RT-qPCR. MM, minimal medium without acetate. Data represent mean ±

SD (*n*=3).

Heterologous expression of *CrLACS1*, *CrLACS2* and *CrLACS3* each recovered the ability of the yeast *faa1 faa4* double mutant to grow on FFAs

To validate the function of *CrLACS* genes, their coding sequences were each introduced into the *Saccharomyces cerevisiae* strain YB525 for complementation. YB525, disrupted in the two LACS-coding genes *FAA1* and *FAA4*, is unable to grow with exogenous free fatty acids (FFAs) as the sole carbon source and thus has been used for functional studies of putative *LACS* genes (Knoll *et al.*, 1995). Eight FFAs were examined, with the carbon chain length ranging from 14 to 20 and the double bonds from 0 to 5. Unlike the control (pYES2) that barely grew, *CrLACS1*, *CrLACS2* and *CrLACS3* all enabled the yeast cells to grow on any of the eight tested FFAs (Fig. 2a), suggesting that their encoded proteins all showed LACS activity when expressed in the yeast. However, the yeast strains expressing *CrLACS2* and *CrLACS3* achieved comparable cell densities and were considerably greater than that expressing *CrLACS1*, indicating CrLACS2 and CrLACS3 may possess stronger enzymatic activities than CrLACS1.

The recombinant CrLACS1, CrLACS2 and CrLACS3 all exhibited acyl-CoA synthetase activities

To gain direct evidence with respect to the activity and substrate preference of CrLACSs, each recombinant CrLACS protein expressed in *E. coli* was purified for *in vitro* enzymatic activity assays, using the above-mentioned FFAs as substrates (Fig. 2b,c). Consistent with the FFA feeding experiments (Fig. 2a), CrLACS2 and CrLACS3 had comparable enzymatic activities and were superior to CrLACS1 regardless of the FFA substrates (Fig. 2c). It is worth noting here that each of CrLACS1, CrLACS2 and CrLACS3 had activities on all eight tested FFAs and exhibited little substrate preference (Fig. 2c). This forms clear contrast to the *C. zofingiensis* LACS isozymes which showed distinct substrate (i.e. FFAs) preferences both *in vitro* and in the yeast

complementation experiment (Wu *et al.*, 2020).

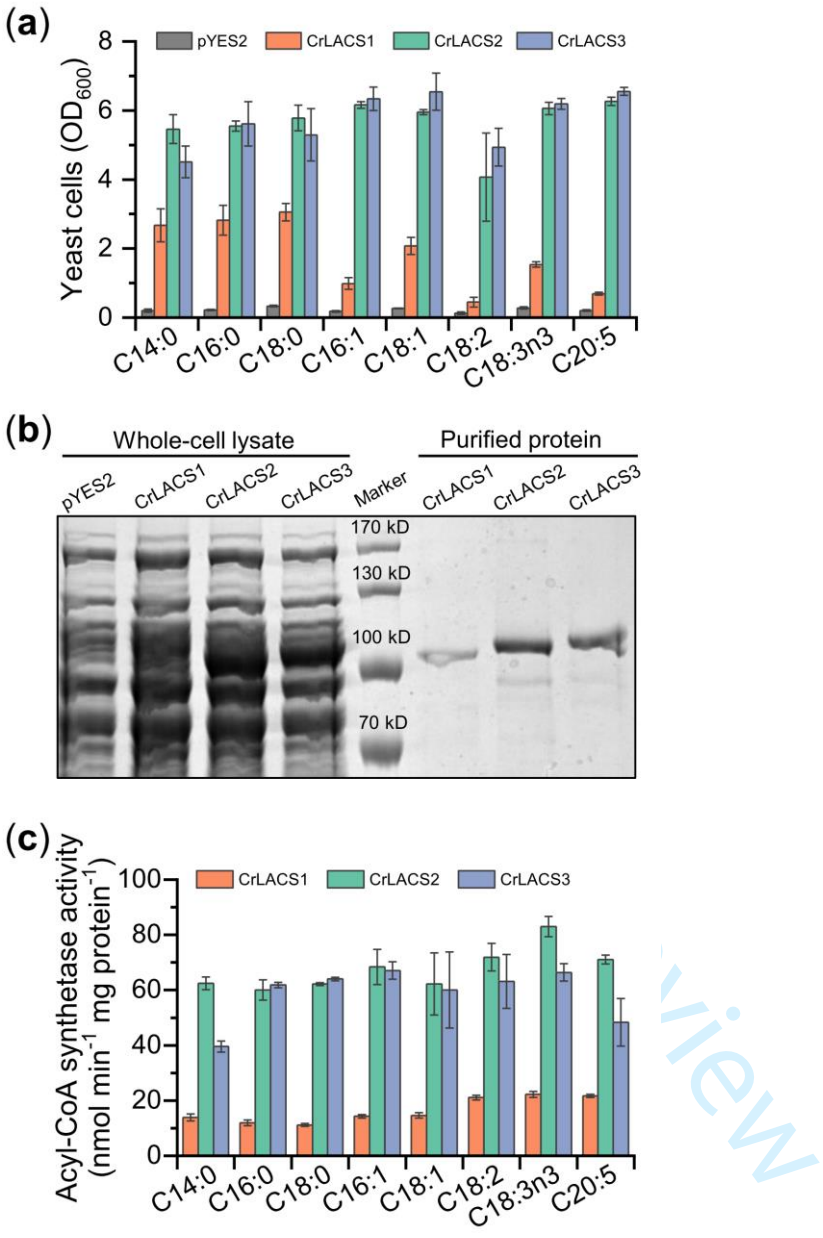

Fig. 2 Functional characterization of CrLACS1, CrLACS2 and CrLACS3. (a) Growth of YB525 cells carrying the empty vector pYES2 or *CrLACS* genes fed on various free fatty acids (FFAs). Yeast growth was recorded at OD 600 nm after 10 days of cultivation. (b) SDS-PAGE separation of recombinant CrLACS1, CrLACS2 and CrLACS3 proteins from *E. coli*. (c) *In vitro* enzymatic assay of CrLACS proteins on various FFAs. Data in (a, c) represent mean ± SD (n=3).

Molecular characterization of insertional mutants of CrLACS1 and CrLACS3

We further investigated the functions of the three LACSs in Chlamydomonas via analysis of insertional mutants. Several insertional lines for each of *CrLACS1*, *CrLACS2 and CrLACS3* could be identified in the Chlamydomonas mutant library (CLIP collection) (Li *et al.*, 2016). Two putative mutants for *CrLACS1*, LMJ.RY0402.129310 (*crlacs1-1*) and LMJ.RY0402.173140 (*crlacs1-2*) were selected for molecular characterization. Using genomic DNA as the template, PCR amplification and Sanger sequencing confirmed insertion of the cassette (with intact 5' and 3' ends) in sense orientation in the first exon of *CrLACS1* for *crlacs1-1* (Fig. 3a, b) and in antisense orientation in the ninth exon for *crlacs1-2* (Fig. S3a, b). Compared to WT, *crlacs1-1* and *crlacs1-2* had ~15.4-fold and 9.0-fold lower *CrLACS1* transcript, respectively (Fig. 3c and Fig. S3c).

Since the *CrLACS2* mutant LMJ.SG0182.015843 had been characterized previously (Li *et al.*, 2016), it, after further molecular confirmation (Fig. S4), was designated as *crlacs2-1* here and used for growth and lipid analyses in our study. As for *CrLACS3*, LMJ.RY0402.199483 (*crlacs3-1*) was chosen for molecular characterization. Although genomic PCR amplification suggested insertion in the expected sites of *CrLACS3*, the 5' and 3' ends of the cassette were not recovered (Fig. 3d, e). This may be due to deletions in the junctions between the cassette and insertion site (Li *et al.*, 2016). Nevertheless, ~5.5-fold decrease of *CrLACS3* transcript was observed in *crlacs3-1* as compared with WT (Fig. 3f).

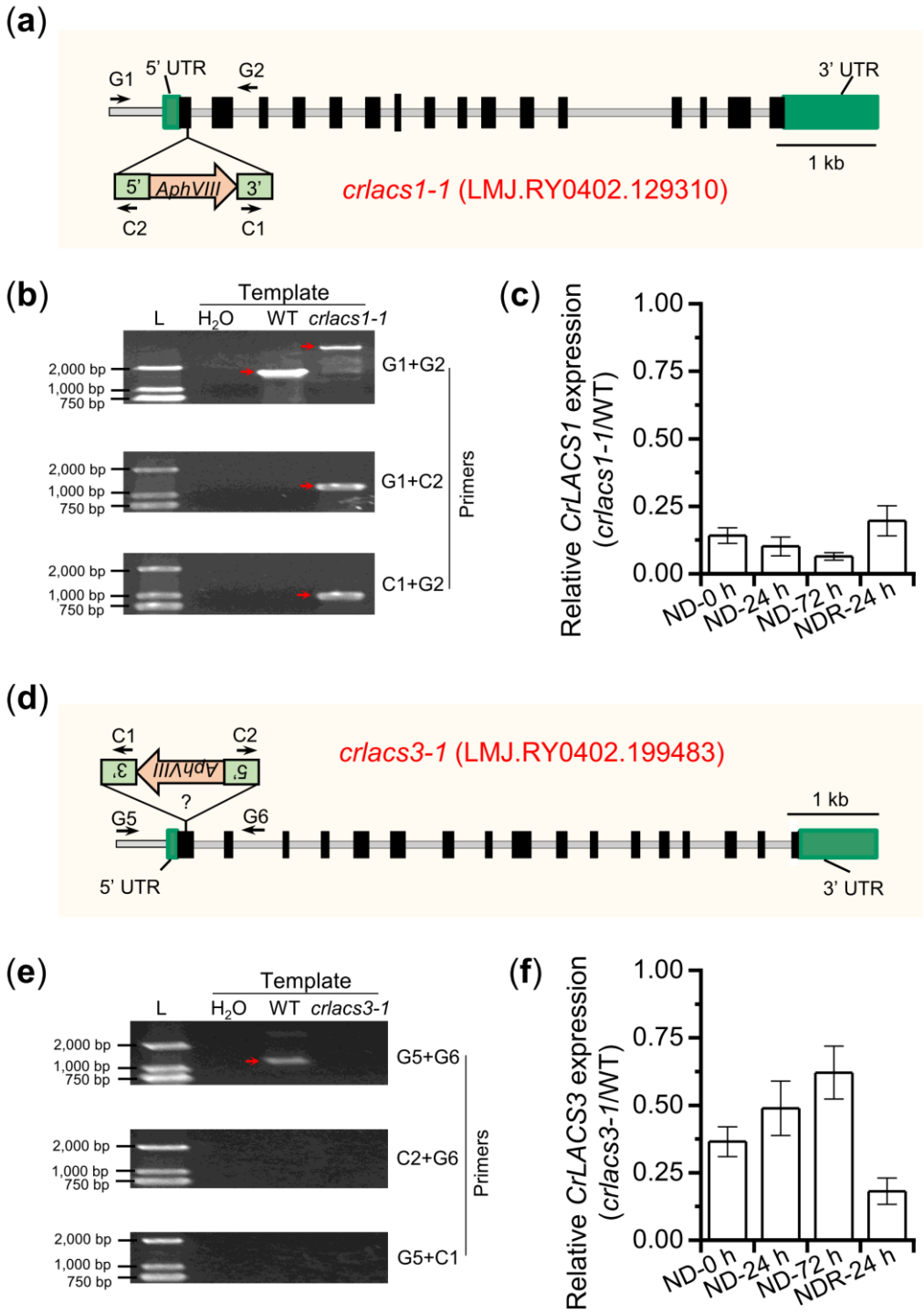

Fig. 3 Molecular characterization of the insertional mutants *crlacs1-1* and *crlacs3-1*. (a, b) Schematic map (a) and PCR validation (b) of the insertion site in *CrLACS1* for *crlacs1-1*. (c) Transcriptional levels of *CrLACS1* in *crlacs1-1* relative to WT. (d, e) Schematic map (d) and PCR validation (e) of the insertion site in *CrLACS3* for *crlacs3-1*. (f) Transcriptional levels of *CrLACS3* in *crlacs3-1* relative to WT. Arrows in (a, d)

designate primers used for validating insertion of the cassette. Data in (c, f) represent mean ± SD (*n*=3).

CrLACS1 or _CrLACS2_ suppression attenuated TAG synthesis under N-deprivation

There was no obvious difference in growth between *crlacs1-1* and WT under NR or ND condition, as indicated by the almost identical cell density (Fig. 4a) and dry weight per 10^6 cells or per mL (Fig. S5a). In response to NDR, cell division was followed and we observed that *crlacs1-1* reached a lower cell density than WT, suggesting an impaired cell division in the mutant (Fig. 4a). Accordingly, *crlacs1-1* had a greater dry weight per cell than WT under this condition (Fig. S5a). TFA and TAG contents rose upon ND and recovered upon NDR in both *crlacs1-1* and WT (Fig. 4b, c). It is worth noting here that *CrLACS1* suppression caused a reduction in both TFA and TAG contents under ND (day 3), but not under NR (day 3); the difference was also noticed under NDR condition (Fig. 4b, c). As such, *crlacs1-1* had a weaker green fluorescence intensity than WT when stained with the neutral lipids specific dye Bodipy (Fig. 4d).

Interestingly, albeit *crlacs1-1* had a lower TAG content than WT under NDR condition, they showed little difference in the TAG remobilization rate as revealed by the comparable percentage of remaining TAG (normalized to TAG content on day 3 of ND) (Fig. 4e). Nevertheless, the total amount of TAG being remobilized was less in the mutant compared to WT, explaining the reduced capacity in cell regrowth in the mutant.

In addition, regardless of the culture conditions, only slight variations were observed between *crlacs1-1* and WT in the fatty acid composition of either TFA or TAG (Fig. S6), consistent with the unbiased preference of CrLACS1 for FFAs (Fig. 1c). The second mutant allele *crlacs1-2* showed similar phenotypes e.g. lower TFA and TAG levels than WT (Fig. S3d). Taken together, our data demonstrated that CrLACS1 is involved in TAG biosynthesis rather than TAG catabolism in Chlamydomonas.

Similarly, the growth of *crlacs2-1* was comparable to WT under NR and ND conditions but was lower than WT under NDR condition (Fig. S7a). Moreover, *crlacs2-1* exhibited lower TFA and TAG contents than WT under ND (day 3) and NDR

conditions (Fig. S7b-d), yet little difference was observed between them in the fatty acid composition of either TFA or TAG (Fig. S8) and in the TAG remobilization ability (Fig. S7e). In this context, *CrLACS2*, resembling *CrLACS1*, contributes to TAG biosynthesis instead of TAG catabolism.

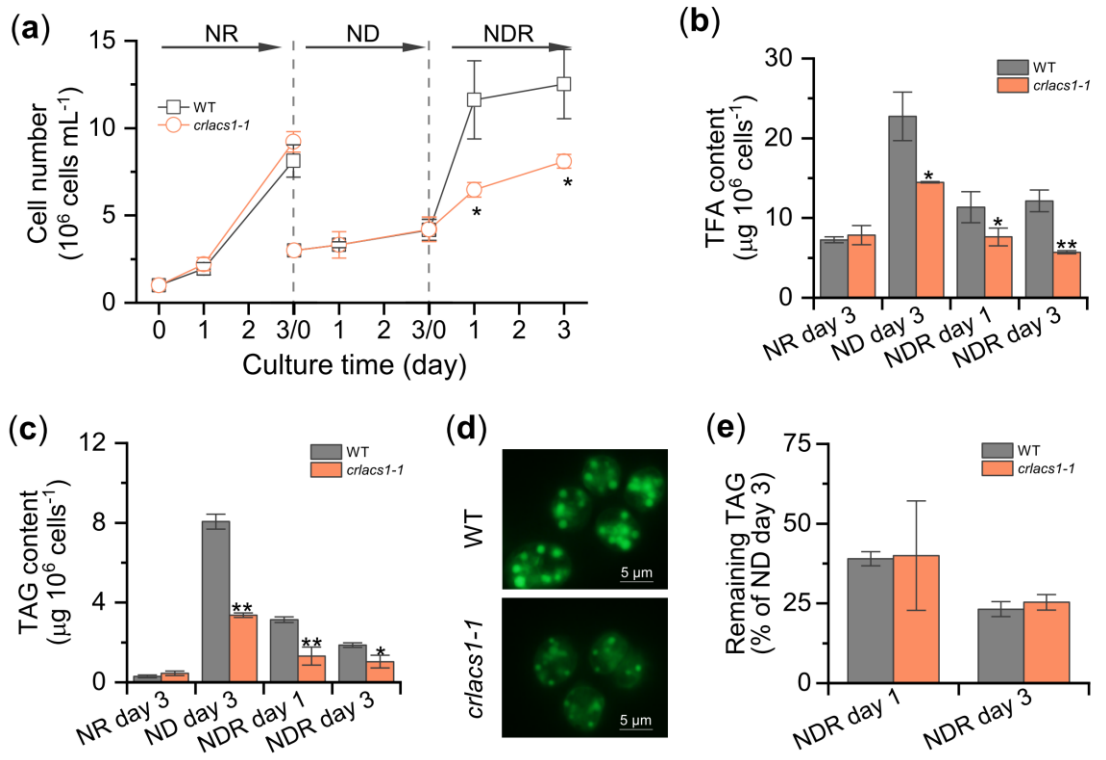

Fig. 4 Comparison of growth and lipids between WT and *crlacs1-1* cells under NR, ND and NDR conditions. (a) Cell number per mL. (b) TFA content. (c) TAG content. (d) Fluorescent microscopy observation of Bodipy-stained algal cells (ND day 3). Green signals indicate lipid droplets. (e) Percentage of remaining TAG under NDR conditions (relative to ND day 3). Data in (a-c, f) represent mean ± SD (n=3). Asterisks indicate the significant difference (Student's t-test, P<0.05* or P<0.01**).

***CrLACS3* suppression impaired TAG remobilization and cell growth severely during N recovery**

Under NR and ND conditions, *crlacs3-1* and WT had comparable cell density and showed no growth difference; upon NDR, while WT underwent a rapid cell division, *crlacs3-1* was severely impaired and its cell density was kept at a low but relatively stable level during the 3-day NDR period (Fig. 5a). Albeit not significant, *crlacs3-1* had

a slightly higher TFA content than WT during ND period; upon NDR, the difference in TFA content between *crlacs3-1* and WT increased (Figure 5b). TAG content in *crlacs3-1* was also slightly greater than that in WT under ND; upon NDR, while WT exhibited a drastic TAG decrease, *crlacs3-1* was severely impaired in TAG decline i.e. its TAG content was 5.1-fold higher than that in WT on day 3 of NDR (Fig. 5c). The large difference in TAG content under NDR between *crlacs3-1* and WT was also supported by the fluorescence microscopic observation of Bodipy-stained cells (Fig. 5d). *CrLACS3* suppression therefore severely disturbed the TAG remobilization ability, as revealed by the considerably greater percentage of remaining TAG in *crlacs3-1* under NDR (Fig. 5e). Similar to *CrLACS1* or *CrLACS2* (Fig. S6 and S8), *CrLACS3* suppression led to little difference in the fatty acid composition of either TFA or TAG (Fig. S9). Taken together, *CrLACS3*, in contrast to *CrLACS1* or *CrLACS2*, is involved in TAG catabolism instead of TAG biosynthesis in Chlamydomonas.

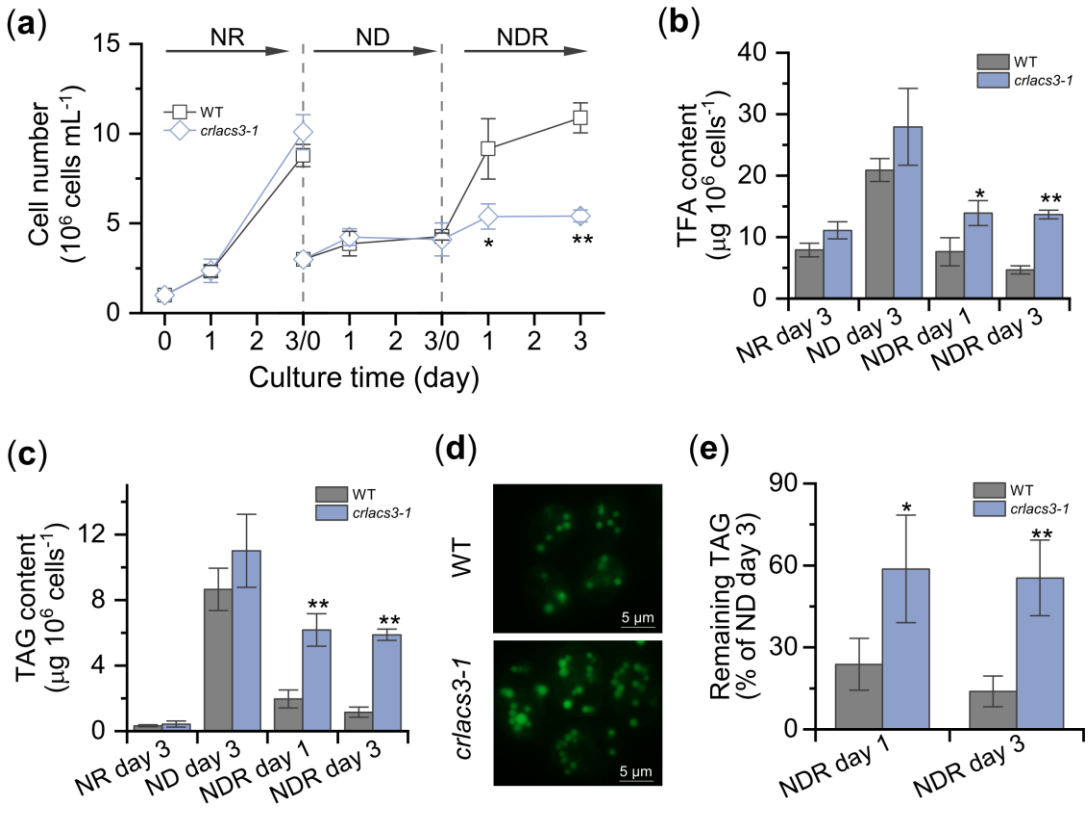

Fig. 5 Comparison of growth and lipids between WT and *crlacs3-1* cells under NR, ND and NDR conditions. (a) Cell number per mL. (b) TFA content. (c) TAG content. (d) Fluorescent microscopy observation of Bodipy-stained algal cells (day 3 of NDR).

Green signals indicate lipid droplets. (e) Percentage of remaining TAG under NDR conditions (relative to ND day 3). Data in (a-c, f) represent mean ± SD (*n*=3). Asterisks indicate the significant difference (Student's *t*-test, $P<0.05$* or $P<0.01$**).

Suppression of CrLACS1 or CrLACS2 but not CrLACS3 led to more galactolipids during N-deprivation

TAG amount in N-deprived Chlamydomonas cells is partly due to *de novo* synthesis and partly due to membrane lipid remodeling. To determine how the suppression of *CrLACS* genes affected polar membrane lipids, monogalactosyldiacylglycerol (MGDG), digalactosyldiacylglycerol (DGDG), sulfoquinovosyl diacylglycerol (SQDG), phosphatidylglycerol (PG), phosphatidyl inositol (PI), phosphatidylethanolamine (PE) and diacylglycerol trimethylhomoserine (DGTS) were quantified for WT, *crlacs1-1*, *crlacs2-1* and *crlacs3-1*. Under NR condition, only slight/little differences in the contents of polar lipids were observed between WT and the mutants (Fig. 6a), suggesting that disruption of the individual *CrLACS* genes had limited effect on metabolism of polar lipids under favorable growth conditions. Nevertheless, on day 3 of ND when TAG was induced to accumulate, different responses were observed in the three mutants: compared to WT, both *crlacs1-1* and *crlacs2-1* contained higher levels of chloroplast membrane lipids particularly MGDG and DGDG but not the ER membrane lipids, while *crlacs3-1* exhibited little difference in any of the membrane polar lipids (Fig. 6b). This result suggests that CrLACS1 and CrLACS2 participate in the activation of FFAs, coming from galactolipid hydrolysis, for TAG synthesis; in their absence, TAG amount is reduced, and galactolipid turnover is halted likely as a result of feedback inhibition by the FFAs.

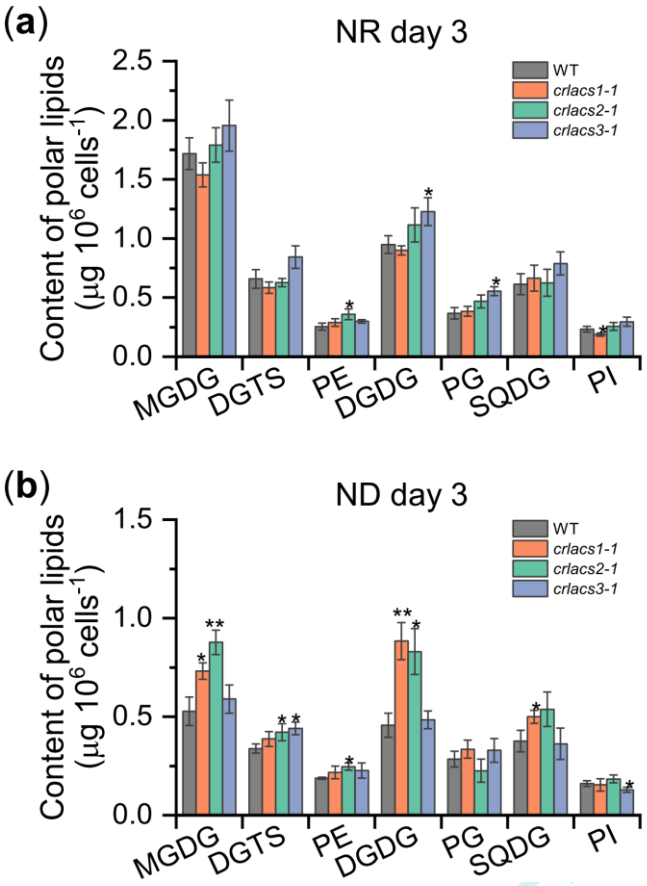

Fig. 6 Contents of membrane lipid classes in WT and mutants under NR and ND conditions. (a) NR day 3. (b) ND day 3. Data represent mean ± SD (n=3). Asterisks indicate the significant difference (Student's t-test, P<0.05* or P<0.01**).

Genetic complementation of *CrLACS1* and *CrLACS3* insertional mutants

To confirm whether the phenotypes of *crlacs1-1* and *crlacs3-1* were caused by suppression of *CrLACS1* and *CrLACS3*, respectively, complementation experiments were performed. Functional complementation of *crlacs2-1* was previously performed (Li *et al.*, 2016) and thus not repeated here. Two independent complemented strains for each mutant were analyzed. Clearly, introduction of *CrLACS1* into *crlacs1-1* restored the transcriptional expression of *CrLACS1* (Fig. 7a), TAG content under ND (day 3) and NDR (day 3) conditions (Fig. 7b), and MGDG and DGDG contents (Fig. 7c), demonstrating firmly that the phenotypes of *crlacs1-1* were due to CrLACS1 dysfunction. Introduction of *CrLACS3* into *crlacs3-1* also led to restoration of *CrLACS1* transcriptional expression (Fig. 7d), TAG content under NDR (day 3)

condition (Fig. 7e) and TAG remobilization ability (Fig. 7f), further confirming the function of CrLACS3 in TAG catabolism in Chlamydomonas.

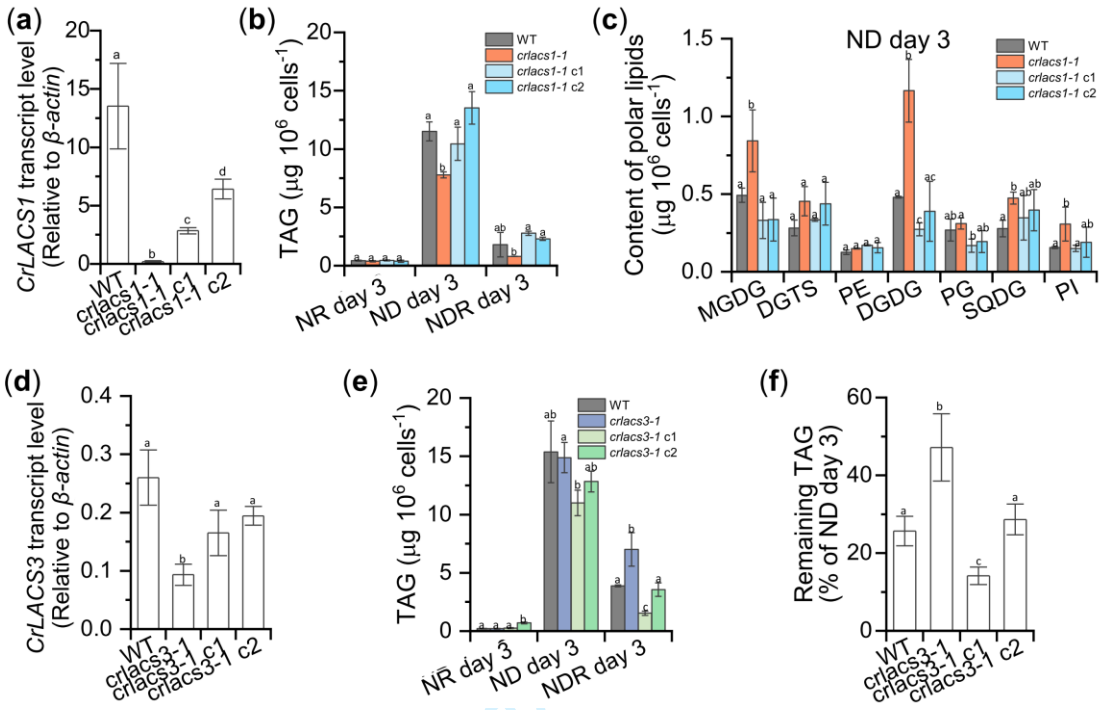

Fig. 7 Complementation of *crlacs1-1* and *crlacs3-1* strains. (a) The transcript levels of *CrLACS1* (relative to *β-actin*) in WT, *crlacs1-1* and the complemented strains on day 3 of ND as determined by RT-qPCR. (b) TAG contents in WT, *crlacs1-1* and the complemented strains under NR, ND and NDR conditions. (c) Contents of polar lipids in WT, *crlacs1-1* and the complemented strains on day 3 of ND. (d) The transcript levels of *CrLACS3* (relative to *β-actin*) in WT, *crlacs3-1* and the complemented strains on day 3 of NDR as determined by RT-qPCR. (e) TAG contents in WT, *crlacs3-1* and the complemented strains under ND and NDR conditions. (f) Percentage of remaining TAG on day 3 of NDR (relative to ND day 3) in WT, *crlacs3-1* and the complemented strains. Data represent mean ±SD (n=3). Different letters above the bars in each group indicate significant difference ($p<0.05$), based on one-way analysis of variance (ANOVA) and Tukey's honestly significant difference (HSD) test.

Comparative transcriptomic analysis between mutants and WT

To understand the transcriptional responses caused by insertional suppression of

CrLACS genes, comparative RNA sequencing (RNA-seq) analysis was performed for WT, *crlacs1-1* and *crlacs2-1* under ND condition and for WT and *crlacs3-1* under NDR condition. Ten high-quality transcriptomes were generated and the biological duplicates within each group showed a high consistence and distinguished from other groups as indicated by the Pearson correlation and principal component analysis (Fig. S10a, b). Over 17,000 genes were mapped and the majority of them had a FPKM value no less than 1 (Fig. S10c and Data S1). Although significant changes occurred for TAG in *crlacs1-1* and *crlacs2-1* under ND conditions (Fig. 4 and Fig. S7) and in *crlacs3-1* under NDR conditions (Fig. 5), the majority of genes involved in lipid metabolic pathways such as *de novo* fatty acid synthesis, fatty acid desaturation, membrane lipid synthesis and turnover (e.g., the MGDG lipase PLASTID GALACTOGLYCEROLIPID DEGRADATION1 - PGD1), TAG assembly and degradation (e.g., the TAG lipase LIP4), and fatty acid β-oxidation (e.g., the acyl-CoA oxidase 2 - ACX2) showed only slight transcriptional variations as compared with WT (Data S2). Likely, the phenotypes of *crlacs1-1*, *crlacs2-1* and *crlacs3-1* observed at the level of lipid classes are therefore mainly attributed to metabolic adjustment rather than transcriptional reprogramming.

Discussion

CrLACS1, CrLACS2 and CrLACS3 are bona fide long-chain acyl-CoA synthetases with activity on a broad range of FFAs

In this study, we demonstrated clearly that CrLACS1, CrLACS2 and CrLACS3 are bona fide LACS enzymes and have overlapping activities in activating FFAs (Fig. 1c). Albeit CrLACS1 has considerably lower activities than CrLACS2 or CrLACS3, they all are functional on a broad range of FFAs without obvious substrate preference. By contrast, in *C. zofingiensis*, an oleaginous green alga closely related to Chlamydomonas (Zhang *et al.*, 2021), the LACS enzymes exhibit distinct preference on FFAs with different carbon chain length and double bonds (Wu *et al.*, 2020). Specifically, CzLACS2, a close homolog of CrLACS2 with 59.5% sequence identity, acts on

saturated and monounsaturated fatty acids yet has little activities on polyunsaturated fatty acids. This suggests that even being phylogenetically closely related, LACS homologues from different algal species may vary greatly in their substrate preference. On the other hand, CzLACS5, a close homolog of CrLACS3 with 69.6% sequence identity, resembles CrLACS3 and acts on a broad range of FFAs. As both Chlamydomonas and *C. zofingiensis* harbor only one peroxisomal LACS isoform (Li-Beisson *et al.*, 2015; Wu *et al.*, 2020), it is not surprising that they did not show particular substrate preference, which is important in ensuring the catabolism of all FFAs by the fatty acid β-oxidation in the peroxisomes.

CrLACS1 and CrLACS2 functionally overlap in TAG biosynthesis and participate in allocation of acyl chains between TAG and galactolipids

LACS is known to participate in a variety of anabolic and catabolic pathways related to acyl-lipid metabolism (DiRusso & Black, 1999; Coleman *et al.*, 2002; Watkins & Ellis, 2012; Zhao *et al.*, 2019). In Chlamydomonas, upon N-deprivation, a stimulus widely used for inducing TAG accumulation, our RT-qPCR results showed that both *CrLACS1* and *CrLACS2* were considerably up-regulated (Fig. 1d), consistent with large-scale RNA-seq studies (Miller *et al.*, 2010; Boyle *et al.*, 2012; Blaby *et al.*, 2013; Goodenough *et al.*, 2014; López García de Lomana *et al.*, 2015). Moreover, when N-deprivation stress was removed (NDR condition), TAG level declined, accompanied by the transcriptional down-regulation of *CrLACS1* and *CrLACS2* (Fig. 1c, d). These correlations point to the potential involvement of *CrLACS1* and *CrLACS2* in TAG biosynthesis. As a strong support, it has been reported that insertional mutation of *CrLACS2* impaired TAG level in Chlamydomonas under N-deprivation condition (Li *et al.*, 2016). Nevertheless, it did not block TAG accumulation; instead, about half of TAG was maintained, suggesting that additional *LACS* gene(s) are involved in TAG biosynthesis in Chlamydomonas. In the present study, we quantified TAG levels in *CrLACS1* mutants as well as the complemented strains (Fig. 4c and 7b), and the results firmly demonstrated that CrLACS1 is also involved in TAG biosynthesis. Although

CrLACS1 has weaker *in vitro* enzymatic activities than CrLACS2 (Fig. 1c), its greater transcriptional increase upon N-deprivation (Fig. 2d) may have boosted their activities substantially. Considering that suppression of CrLACS1 or CrLACS2 led to ~50% TAG reduction, they two likely make comparable contribution to TAG synthesis in Chlamydomonas and function independently of each other. In accord with this, at least at the transcriptional level, neither *CrLACS1* nor *CrLACS2* disruption stimulated the expression of the other one during N-deprivation (Fig. S11).

We attempted to generate double mutants of *CrLACS1* and *CrLACS2* by genetic crossing, but failed, likely because the double mutants are lethal. It is reasonable as acyl-CoAs produced from the action of CrLACS1 and CrLACS2 also participate in the synthesis of extra-chloroplast membrane lipids (Li-Beisson *et al.*, 2015), which are essential for cell survival. While suppression of *CrLACS1* or *CrLACS2* attenuated TAG levels on day 3 of N-deprivation (Fig. 4c and Fig. S6c), the ER membrane lipids DGTS, PE and PI showed little variations (Fig. 6b). This is not surprising considering that during N-deprivation, membrane lipid syntheses were halted thus there is little requirement for acyl-CoAs. It is worth noting here that in comparison with WT, both *crlacs1-1* and *crlacs2-1* maintained higher levels of the chloroplast lipids MGDG and DGDG under N-deprivation (Fig, 6b), pointing to a role of CrLACS1 and CrLACS2 in allocating acyl chains between TAG and chloroplast lipids particularly galactolipids. These results also support that galactolipid remodeling contributes fatty acids for TAG biosynthesis in Chlamydomonas, in line with the previous study where the insertional mutation of *PGD1* gene that encodes a MGDG lipase impairs TAG accumulation (Li *et al.*, 2012b). The fatty acids either *de novo* synthesized or recycled from chloroplast lipids, prior to incorporation into TAG, have to be exported out of the chloroplast and activated by LACS enzymes. It has been reported that LACS, coupled with a fatty acid transporter, is involved in transporting FFAs into the cytoplasm of bacteria and yeast cells (DiRusso & Black, 1999; Zou *et al.*, 2003). Similarly, in land plants and algae, LACS probably functions with a fatty acid transporter (FAX1) localized at the chloroplast envelop (Li *et al.*, 2015; Li *et al.*, 2019) and facilitate transport of FFAs

from the chloroplast to the cytoplasm. In this context, suppression of *CrLACS1* or *CrLACS2* may impair export of FFAs out the chloroplast, which attenuates galactolipid turnover (e.g., mediated by PGD1) and hydrolysis of acyl-ACPs (i.e., catalyzed by the acyl-ACP thioesterase FAT1) via the possible product feedback inhibition by the FFAs (Fig. 8). Accordingly, more acyl-ACPs may be rerouted to chloroplast membrane lipids. Nevertheless, the transcriptional levels of *PGD1*, *FAT1*, or *FAX1* were not down-regulated in *crlacs1-1* or *crlacs2-1* as compared to WT (Data S2), indicating that the lipid phenotypes are likely due to a shift in metabolic adjustment rather than transcriptional reprogramming. It has been reported in Arabidopsis that impairing export of FFAs out the chloroplast also causes increased levels of certain chloroplast membrane lipids at the expense of TAG (Li *et al.*, 2015).

Nevertheless, when Chlamydomonas grew during N-replete condition and it synthesized a basal level of TAG, neither TAG nor any of the chloroplast membrane lipids was impacted by *CrLACS1* or *CrLACS2* suppression (Fig. 4c, 6a and S7c). We examined expression of *CrLACS* genes under N-replete condition in *crlacs1-1* and *crlacs2-1*; interestingly, *CrLACS1* suppression caused a 5.1-fold increase of *CrLACS2* transcript while *CrLACS2* suppression led to a 2.2-fold increase of *CrLACS1* transcript (Fig. S11). In other words, when the individual *CrLACS1* or *CrLACS2* is inactivated, Chlamydomonas can adopt a compensation strategy to maintain lipid homeostasis by stimulating expression of the other. It is worth mentioning that this compensation strategy occurs under N-replete but not N-deprivation (Fig. S11), indicating a fine temporal collaboration between *CrLACS1* and *CrLACS2*. Of course, we cannot exclude the possibility that the acyl-CoA independent pathway mediated by the phospholipid:diacylglycerol acyltransferase (PDAT) could be further stimulated to make TAG in response to *CrLACS1* or *CrLACS2* disruption under N-replete condition, as the Chlamydomonas PDAT is known to preferentially function under favorable growth conditions (Yoon *et al.*, 2012).

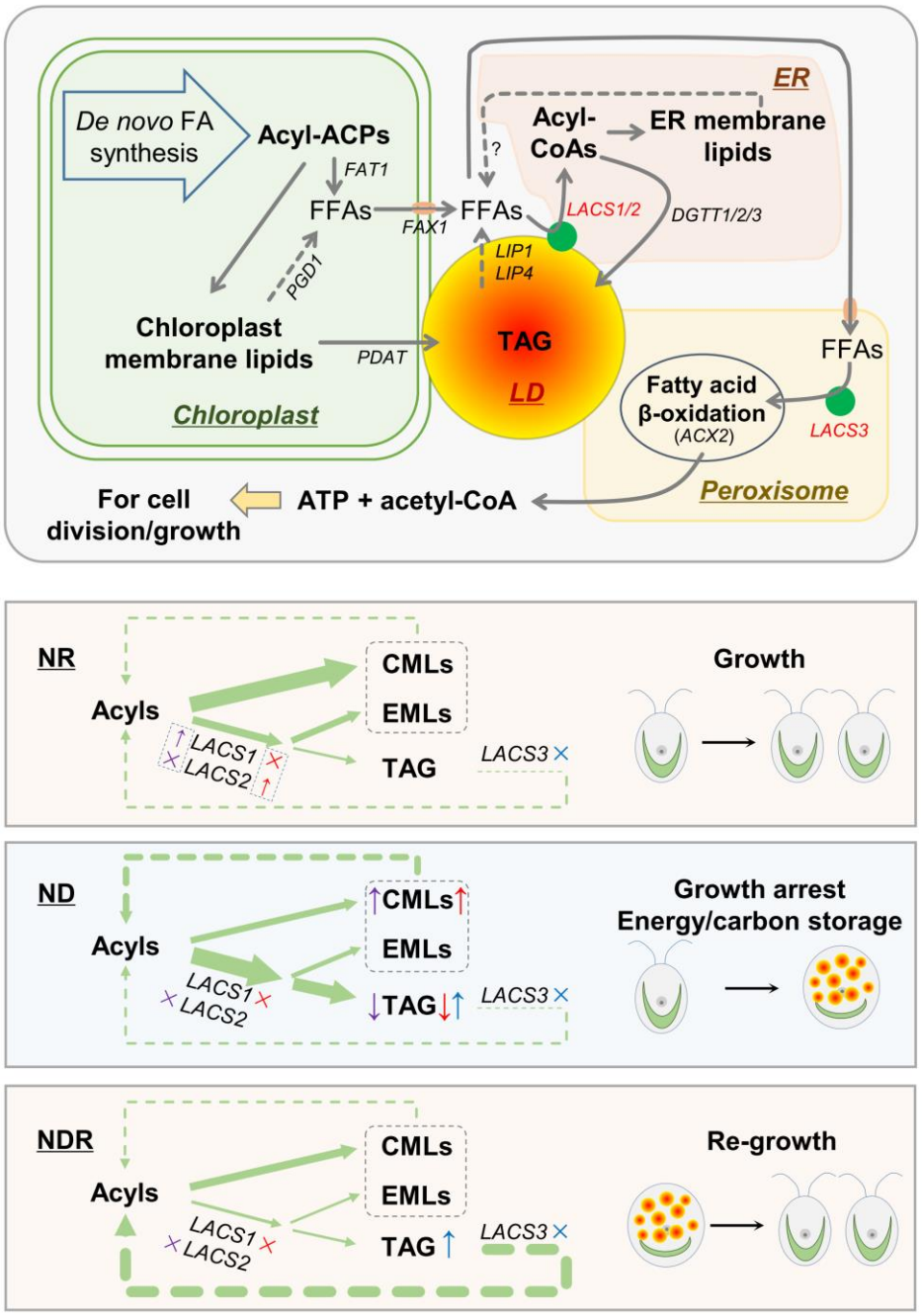

Fig. 8 Proposed model explaining that CrLACS1, CrLACS2 and CrLACS3 function spatially and temporally to achieve lipid homeostasis for growth and energy storage in Chlamydomonas. Multiple organelles are involved in lipid metabolism, including the chloroplast, ER, LDs and peroxisomes, etc. CrLACS1 and CrLACS2 reside in the ER and/or LDs, and contribute to TAG biosynthesis, while CrLACS3 is localized in peroxisomes and contributes to TAG degradation. Under NR condition, growth is active for cell reproduction; acyls are allocated predominantly to chloroplast membrane lipids

(CMLs) and ER membrane lipids (EMLs), with a basal level of TAG. Under ND condition, growth is arrested; membrane lipid remodeling and TAG biosynthesis are stimulated while TAG catabolism is minimized, leading to massive accumulation of TAG for energy and carbon storage. Suppression of *CrLACS1* and *CrLACS2* each impairs TAG accumulation with increased levels of CMLs particularly MGDG and DGDG. Exposing ND-treated cells to NDR condition, TAG biosynthesis is minimized while TAG catabolism is stimulated, resulting in TAG degradation to supply carbon and energy sources for cell re-growth. *CrLACS3* suppression severely impairs TAG degradation and thus the cell re-growth. The thickness of green arrows refer to acyl fluxes (not on scale).

CrLACS3 plays a critical role in TAG remobilization to support cell growth

In Chlamydomonas, fatty acid β-oxidation occurs in peroxisomes, which play a critical role in remobilizing the energy-dense TAG and providing energy and carbon precursors for cell division (Kong *et al.*, 2017; Kong *et al.*, 2018; Lee *et al.*, 2020). *CrLACS3* suppression severely impaired TAG degradation and allowed the alga to maintain high levels of TAG during N-recovery (Fig. 5c). CrLACS3, predicted to reside in peroxisomes based on homology to other known LACS proteins, thus connects TAG degradation to fatty acid β-oxidation by activating FFAs released from TAG and DAG that are catalyzed by LIP4 (Warakanont *et al.*, 2019) and LIP1 (Li *et al.*, 2012a), respectively (Fig. 8). Moreover the defects in TAG catabolism is accompanied by a near total block in cell growth (Fig. 5a), suggesting a critical role of *CrLACS3* in TAG remobilization for supporting cell division when the adverse conditions are relieved. It is worth mentioning here that in *crlacs3-1* TAG remobilization was not completely blocked, which is most likely due to the fact that *crlacs3-1* is only a knock-down rather than a knock-out mutant. The function of CrLACS3 is further supported by its dynamic expression pattern at the transcriptional level during varying N status (Fig. 2d). Moreover, the expression profile of *CrLACS3* also agrees with the transcriptional expression patterns of known lipolytic enzymes such as LIP4 and LIP1 or the known

peroxisomal ACX2 that catalyzes the first step of fatty acid β-oxidation in Chlamydomonas (Li *et al.*, 2012b; Kong *et al.*, 2017; Warakanont *et al.*, 2019). These points to an orchestrated transcriptional control of TAG remobilization.

The remobilization of TAG to provide carbon and energy sources for cell regrowth is reflected by suppression of not only *CrLACS3* but also *CrLACS1* or *CrLACS2*. Under N-deprivation (ND day 3), both *crlacs1-1* and *crlacs2-1* have lower amounts of TAG than the WT (Fig.4c and Fig. S7c). When subjected to N-recovery, although the TAG remobilization rate is not affected, the amounts of remobilized TAG in *crlacs1-1* and *crlacs2-1* are smaller than that in WT (Fig.4e and Fig. S7e). Therefore, less carbon and energy sources are available for the mutants, leading to impaired cell growth (Fig.4a and Fig. S7a).

CrLACS1, CrLACS2 and CrLACS3 collaborate spatially and temporally in lipid homeostasis

Multiple organelles are involved in lipid metabolism, including chloroplast, ER, LDs and peroxisomes. Serving as connections among these organelles, CrLACS1, CrLACS2 and CrLACS3 function spatially and temporally for fine collaboration to maintain lipid homeostasis in Chlamydomonas (Fig. 8). CrLACS1 and CrLACS2, residing in the ER and/or LDs, function in activating fatty acids to support the biosynthesis of ER membrane lipids as well as of a basal level of TAG under favorable growth conditions. Suppressing each of *CrLACS1* and *CrLACS2* would trigger transcriptional up-regulation of the other one for compensation thus avoiding disturbance in membrane lipid biosynthesis and cell growth. Once exposed to nutrient depletion, e.g., N-deprivation, *CrLACS1* and *CrLACS2* are substantially induced to provide enough acyl-CoAs for the ER-localized acyltransferases such as type II diacylglycerol acyltransferases (DGTT1/2/3); the peroxisome-localized CrLACS3, on the other hand, is maintained at a basal level to minimize fatty acid β-oxidation, thus allowing massive accumulation of TAG in Chlamydomonas. CrLACS1 and CrLACS2 function redundantly yet both are indispensable for TAG synthesis, which is packed

into the ER-derived LDs for storage. During N-recovery, CrLACS3 is triggered to express to a very high level and acts in concert with TAG/DAG lipases (e.g., LIP4 and LIP1) and fatty acid β-oxidation enzymes (e.g., ACX2) to remobilize TAG for supplying energy and carbon for cell division and algal growth.

Biotechnological implications

We here have demonstrated the functionality of CrLACSs: CrLACS1 and CrLACS2 are involved in providing acyl-CoAs for TAG synthesis, while *CrLACS3* provides acyl-CoAs in peroxisomes to enter fatty acid β-oxidation. These three CrLACS proteins are therefore promising targets of genetic engineering to manipulate TAG accumulation in algae. *CrLACS3* suppression has led to an increase in TAG level in Chlamydomonas (Fig. 5c), which together with overexpression of *CrLACS1* or *CrLACS2* would have the potential to further promote TAG accumulation. For the time being, we have confirmed that heterologous expression of *CrLACS1* or *CrLACS2* promoted both TFA and TAG levels in yeast (Fig. S12). These two genes may be applied to oleaginous algae for TAG enhancement, as is the case of *CzLACS2* expressed in *Nannochloropsis oceanica* (Wu *et al.*, 2020). Moreover, CrLACS enzymes particularly CrLACS2 possess strong activities on eicosapentaenoic acid (EPA), a high-value compound beneficial to human health (Lupette & Benning, 2020), and the activity (Fig. 1c) reaches over 10-fold greater than that of CzLACSs (Wu *et al.*, 2020). They can be overexpressed in *N. oceanica*, together with the acyltranserases that have potent activities in incorporating EPA into TAG (Liu *et al.*, 2016a; Mao *et al.*, 2019), for the purposes of not only promoting TAG accumulation but also enriching EPA in TAG.

Acknowledgements

We thank Dr. Xiaobo Li at Westlake University, China for his recommendation on using the *CrLACS2* knockout mutant LMJ.SG0182.015843. This work is partially supported by grants from the National Natural Science Foundation of China (31770048) and the National Key R&D Program of China (2018YFA0902500).

689

690 **Author contributions**

691 FB carried out the main experiments and analyzed the data; LY performed algal
692 cultivation and lipid analysis; JS maintained algal strains and performed algal
693 cultivation; YL-B gave critical comments and revised the paper; JL conceived the
694 idea, designed the research, analyzed the data and wrote the paper.

695

696 **Data Availability Statement**

697 The authors confirm that the data supporting the findings of this study are available
698 within the article and its supplementary materials

References

Ayaz A, Saqib S, Huang H, Zaman W, Lü S, Zhao H. 2021. Genome-wide comparative analysis of long-chain acyl-CoA synthetases (LACSs) gene family: A focus on identification, evolution and expression profiling related to lipid synthesis. *Plant Physiology and Biochemistry* **161**: 1-11.

Blaby IK, Glaesener AG, Mettler T, Fitz-Gibbon ST, Gallaher SD, Liu B, Boyle NR, Kropat J, Stitt M, Johnson S, et al. 2013. Systems-level analysis of nitrogen starvation–induced modifications of carbon metabolism in a *Chlamydomonas reinhardtii* starchless mutant. *The Plant Cell* **25**: 4305-4323.

Black PN, DiRusso CC, Metzger AK, Heimert TL. 1992. Cloning, sequencing, and expression of the *fadD* gene of *Escherichia coli* encoding acyl coenzyme A synthetase. *Journal of Biological Chemistry* **267**: 25513-25520.

Boyle NR, Page MD, Liu B, Blaby IK, Casero D, Kropat J, Cokus SJ, Hong-Hermesdorf A, Shaw J, Karpowicz SJ, et al. 2012. Three acyltransferases and nitrogen-responsive regulator are implicated in nitrogen starvation-induced triacylglycerol accumulation in *Chlamydomonas*. *Journal of Biological Chemistry* **287**: 15811-15825.

Coleman RA, Lewin TM, Van Horn CG, Gonzalez-Baró MR. 2002. Do long-chain acyl-CoA synthetases regulate fatty acid entry into synthetic versus degradative pathways? *The Journal of Nutrition* **132**: 2123-2126.

De Carvalho CCCR, Caramujo MJ. 2018. The various roles of fatty acids. *Molecules* **23**.

DiRusso CC, Black PN. 1999. Long-chain fatty acid transport in bacteria and yeast. Paradigms for defining the mechanism underlying this protein-mediated process. *Molecular and Cellular Biochemistry* **192**: 41-52.

Færgeman NJ, Black PN, Zhao XD, Knudsen J, DiRusso CC. 2001. The acyl-CoA synthetases encoded within *FAA1* and *FAA4* in *Saccharomyces cerevisiae* function as components of the fatty acid transport system linking import, activation, and intracellular utilization. *Journal of Biological Chemistry* **276**:

37051-37059.

Fulda M, Schnurr J, Abbadi A, Heinz E, Browse J. 2004. Peroxisomal acyl-CoA synthetase activity is essential for seedling development in *Arabidopsis thaliana*. *The Plant Cell* **16**: 394-405.

Fulda M, Shockey J, Werber M, Wolter FP, Heinz E. 2002. Two long-chain acyl-CoA synthetases from Arabidopsis thaliana involved in peroxisomal fatty acid β-oxidation. *The Plant Journal* **32**: 93-103.

Glatz JFC, Luiken JJFP. 2015. Fatty acids in cell signaling: Historical perspective and future outlook. *Prostaglandins, Leukotrienes and Essential Fatty Acids* **92**: 57-62.

Goodenough U, Blaby I, Casero D, Gallaher SD, Goodson C, Johnson S, Lee J-H, Merchant SS, Pellegrini M, Roth R, et al. 2014. The path to triacylglyceride obesity in the *sta6* strain of *Chlamydomonas reinhardtii*. *Eukaryotic Cell* **13**: 591-613.

Guo X, Jiang M, Wan X, Hu C, Gong Y. 2014. Identification and biochemical characterization of five long-chain acyl-coenzyme A synthetases from the diatom *Phaeodactylum tricornutum*. *Plant Physiology and Biochemistry* **74**: 33-41.

Hettema EH, van Roermund CW, Distel B, van den Berg M, Vilela C, Rodrigues-Pousada C, Wanders RJ, Tabak HF. 1996. The ABC transporter proteins Pat1 and Pat2 are required for import of long-chain fatty acids into peroxisomes of Saccharomyces cerevisiae. *The EMBO Journal* **15**: 3813-3822.

Hu Q, Sommerfeld M, Jarvis E, Ghirardi M, Posewitz M, Seibert M, Darzins A. 2008. Microalgal triacylglycerols as feedstocks for biofuel production: perspectives and advances. *The Plant Journal* **54**: 621-639.

Ichihara K, Shibasaki Y. 1991. An enzyme-coupled assay for acyl-CoA synthetase. *Journal Lipid Research* **32**: 1709-1712.

Ischebeck T, Krawczyk HE, Mullen RT, Dyer JM, Chapman KD. 2020. Lipid droplets in plants and algae: Distribution, formation, turnover and function.

Seminars in Cell & Developmental Biology **108**: 82-93.

Jessen D, Olbrich A, Knüfer J, Krüger A, Hoppert M, Polle A, Fulda M. 2011. Combined activity of LACS1 and LACS4 is required for proper pollen coat formation in Arabidopsis. *The Plant Journal* **68**: 715-726.

Jessen D, Roth C, Wiermer M, Fulda M. 2015. Two activities of long-chain acyl-coenzyme A synthetase are involved in lipid trafficking between the endoplasmic reticulum and the plastid in Arabidopsis. *Plant Physiology* **167**: 351-366.

Jia B, Song Y, Wu M, Lin B, Xiao K, Hu Z, Huang Y. 2016. Characterization of long-chain acyl-CoA synthetases which stimulate secretion of fatty acids in green algae *Chlamydomonas reinhardtii*. *Biotechnology for Biofuels* **9**: 184-184.

Johnson DR, Knoll LJ, Levin DE, Gordon JI. 1994. Saccharomyces cerevisiae contains four fatty acid activation (FAA) genes: an assessment of their role in regulating protein N-myristoylation and cellular lipid metabolism. *Journal Cell Biology* **127**: 751-762.

Kamisaka Y, Tomita N, Kimura K, Kainou K, Uemura H. 2007. *DGA1* (diacylglycerol acyltransferase gene) overexpression and leucine biosynthesis significantly increase lipid accumulation in the Δ*snf2* disruptant of *Saccharomyces cerevisiae*. *Biochemical Journal* **408**: 61-68.

Kindle KL. 1990. High-frequency nuclear transformation of *Chlamydomonas reinhardtii*. *Proceedings of the National Academy of Sciences USA* **87**: 1228-1232.

Knoll LJ, Johnson DR, Gordon JI. 1995. Complementation of *Saccharomyces cerevisiae* strains containing fatty acid activation gene (FAA) deletions with a mammalian acyl-CoA synthetase. *Journal of Biological Chemistry* **270**: 10861-10867.

Kong F, Burlacot A, Liang Y, Légeret B, Alseekh S, Brotman Y, Fernie AR, Krieger-Liszkay A, Beisson F, Peltier G, et al. 2018. Interorganelle communication: Peroxisomal MALATE DEHYDROGENASE2 connects lipid

catabolism to photosynthesis through redox coupling in Chlamydomonas. *The Plant Cell* **30**: 1824.

Kong F, Liang Y, Legeret B, Beyly-Adriano A, Blangy S, Haslam RP, Napier JA, Beisson F, Peltier G, Li-Beisson Y. 2017. *Chlamydomonas* carries out fatty acid beta-oxidation in ancestral peroxisomes using a bona fide acyl-CoA oxidase. *The Plant Journal* **90**: 358-371.

Kong F, Yamaoka Y, Ohama T, Lee Y, Li-Beisson Y. 2019. Molecular genetic tools and emerging synthetic biology strategies to increase cellular oil content in *Chlamydomonas reinhardtii*. *Plant and Cell Physiology* **60**: 1184-1196.

Lauersen K, Kruse O, Mussgnug J. 2015. Targeted expression of nuclear transgenes in *Chlamydomonas reinhardtii* with a versatile, modular vector toolkit. *Applied Microbiology and Biotechnology* **99**: 3491-3503.

Lee J, Yamaoka Y, Kong F, Cagnon C, Beyly-Adriano A, Jang S, Gao P, Kang B-H, Li-Beisson Y, Lee Y. 2020. The phosphatidylethanolamine-binding protein DTH1 mediates degradation of lipid droplets in *Chlamydomonas reinhardtii*. *Proceedings of the National Academy of Sciences USA* **117**: 23131-23139.

Levasseur W, Perré P, Pozzobon V. 2020. A review of high value-added molecules production by microalgae in light of the classification. *Biotechnology Advances* **41**: 107545.

Li-Beisson Y, Beisson F, Riekhof W. 2015. Metabolism of acyl-lipids in *Chlamydomonas reinhardtii*. *The Plant Journal* **82**: 504–522.

Li N, Gügel IL, Giavalisco P, Zeisler V, Schreiber L, Soll J, Philippar K. 2015. FAX1, a novel membrane protein mediating plastid fatty acid export. *PLoS Biology* **13**: e1002053.

Li N, Zhang Y, Meng H, Li S, Wang S, Xiao Z, Chang P, Zhang X, Li Q, Guo L, et al. 2019. Characterization of *Fatty Acid EXporters* involved in fatty acid transport for oil accumulation in the green alga *Chlamydomonas reinhardtii*. *Biotechnology for Biofuels* **12**: 14.

Li X, Benning C, Kuo M-H. 2012a. Rapid triacylglycerol turnover in *Chlamydomonas*

reinhardtii requires a lipase with broad substrate specificity. *Eukaryotic Cell* **11**: 1451-1462.

Li X, Moellering ER, Liu B, Johnny C, Fedewa M, Sears BB, Kuo M-H, Benning C. 2012b. A galactoglycerolipid lipase is required for triacylglycerol accumulation and survival following nitrogen deprivation in *Chlamydomonas reinhardtii*. *The Plant Cell* **24**: 4670-4686.

Li X, Zhang R, Patena W, Gang SS, Blum SR, Ivanova N, Yue R, Robertson JM, Lefebvre PA, Fitz-Gibbon ST, et al. 2016. An indexed, mapped mutant library enables reverse genetics studies of biological processes in *Chlamydomonas reinhardtii*. *The Plant Cell* **28**: 367-387.

Liu J, Han D, Yoon K, Hu Q, Li Y. 2016a. Characterization of type 2 diacylglycerol acyltransferases in *Chlamydomonas reinhardtii* reveals their distinct substrate specificities and functions in triacylglycerol biosynthesis. *The Plant Journal* **86**: 3-19.

Liu J, Mao X, Zhou W, Guarnieri MT. 2016b. Simultaneous production of triacylglycerol and high-value carotenoids by the astaxanthin-producing oleaginous green microalga *Chlorella zofingiensis*. *Bioresource Technology* **214**: 319-327.

Liu J, Sun Z, Mao X, Gerken H, Wang X, Yang W. 2019. Multiomics analysis reveals distinct mechanism of oleaginousness in the emerging model alga *Chromochloris zofingiensis*. *The Plant Journal* **98**: 1060–1077.

López García de Lomana A, Schäuble S, Valenzuela J, Imam S, Carter W, Bilgin DD, Yohn CB, Turkarslan S, Reiss DJ, Orellana MV, et al. 2015. Transcriptional program for nitrogen starvation-induced lipid accumulation in *Chlamydomonas reinhardtii*. *Biotechnology for Biofuels* **8**: 1-18.

Lü S, Song T, Kosma DK, Parsons EP, Rowland O, Jenks MA. 2009. Arabidopsis CER8 encodes long-chain acyl-CoA synthetase 1 (LACS1) that has overlapping functions with LACS2 in plant wax and cutin synthesis. *The Plant Journal* **59**: 553-564.

Lupette J, Benning C. 2020. Human health benefits of very-long-chain polyunsaturated fatty acids from microalgae. *Biochimie* **178**: 15-25.

Mao X, Wu T, Kou Y, Shi Y, Zhang Y, Liu J. 2019. Characterization of type I and type II diacylglycerol acyltransferases from the emerging model alga *Chlorella zofingiensis* reveals their functional complementarity and engineering potential. *Biotechnology for Biofuels* **12**: 28.

Merchant SS, Kropat J, Liu B, Shaw J, Warakanont J. 2012. TAG, You're it! *Chlamydomonas* as a reference organism for understanding algal triacylglycerol accumulation. *Current Opinion in Biotechnology* **23**: 352-363.

Miller R, Wu G, Deshpande RR, Vieler A, Gartner K, Li X, Moellering ER, Zauner S, Cornish AJ, Liu B, et al. 2010. Changes in transcript abundance in *Chlamydomonas reinhardtii* following nitrogen deprivation predict diversion of metabolism. *Plant Physiology* **154**: 1737-1752.

Moellering ER, Benning C. 2010. RNA interference silencing of a major lipid droplet protein affects lipid droplet size in *Chlamydomonas reinhardtii*. *Eukaryotic Cell* **9**: 97-106.

Nguyen HM, Baudet M, Cuiné S, Adriano J-M, Barthe D, Billon E, Bruley C, Beisson F, Peltier G, Ferro M, et al. 2011. Proteomic profiling of oil bodies isolated from the unicellular green microalga *Chlamydomonas reinhardtii*: With focus on proteins involved in lipid metabolism. *Proteomics* **11**: 4266-4273.

Park J-J, Wang H, Gargouri M, Deshpande RR, Skepper JN, Holguin FO, Juergens MT, Shachar-Hill Y, Hicks LM, Gang DR. 2015. The response of *Chlamydomonas reinhardtii* to nitrogen deprivation: a systems biology analysis. *The Plant Journal* **81**: 611-624.

Resh MD. 2016. Fatty acylation of proteins: The long and the short of it. *Progress in Lipid Research* **63**: 120-131.

Schnurr JA, Shockey JM, de Boer GJ, Browse JA. 2002. Fatty acid export from the chloroplast. Molecular characterization of a major plastidial acyl-coenzyme A synthetase from Arabidopsis. *Plant Physiology* **129**: 1700-1709.

Shi Y, Liu M, Ding W, Liu J. 2020. Novel insights into phosphorus deprivation-boosted lipid synthesis in the marine alga *Nannochloropsis oceanica* without compromising biomass production. *Journal of Agricultural and Food Chemistry* **68**: 11488–11502.

Shockey JM, Fulda MS, Browse JA. 2002. Arabidopsis contains nine long-chain acyl-coenzyme A synthetase genes that participate in fatty acid and glycerolipid metabolism. *Plant Physiology* **129**: 1710.

Tang Y, Rosenberg JN, Bohutskyi P, Yu G, Betenbaugh MJ, Wang F. 2016. Microalgae as a feedstock for biofuel precursors and value-added products: Green fuels and golden opportunities. *BioResources* **11**: 2850-2885.

Valledor L, Furuhashi T, Recuenco-Munoz L, Wienkoop S, Weckwerth W. 2014. System-level network analysis of nitrogen starvation and recovery in *Chlamydomonas reinhardtii* reveals potential new targets for increased lipid accumulation. *Biotechnology for Biofuels* **7**: 171.

Wang X, Wei H, Mao X, Liu J. 2019. Proteomics analysis of lipid droplets from the oleaginous alga *Chromochloris zofingiensis* reveals novel proteins for lipid metabolism. *Genomics, Proteomics & Bioinformatics* **17**: 260-272.

Warakanont J, Li-Beisson Y, Benning C. 2019. LIP4 is involved in triacylglycerol degradation in *Chlamydomonas reinhardtii*. *Plant and Cell Physiology* **60**: 1250–1259.

Watkins PA, Ellis JM. 2012. Peroxisomal acyl-CoA synthetases. *Biochimica et Biophysica Acta (BBA) - Molecular Basis of Disease* **1822**: 1411-1420.

Weng H, Molina I, Shockey J, Browse J. 2010. Organ fusion and defective cuticle function in a *lacs1lacs2* double mutant of Arabidopsis. *Planta* **231**: 1089-1100.

Wu T, Fu Y, Shi Y, Li Y, Kou Y, Mao X, Liu J. 2020. Functional characterization of long-chain acyl-CoA synthetase gene family from the oleaginous alga *Chromochloris zofingiensis*. *Journal of Agricultural and Food Chemistry* **68**: 4473-4484.

Yoon K, Han D, Li Y, Sommerfeld M, Hu Q. 2012. Phospholipid:diacylglycerol

acyltransferase is a multifunctional enzyme involved in membrane lipid turnover and degradation while synthesizing triacylglycerol in the unicellular green microalga *Chlamydomonas reinhardtii*. *The Plant Cell* **24**: 3708-3724.

Zhang L, Ma XL, Yang GP, Zhu BH, Han JC, Yu WG, Pan KH. 2012. Isolation and characterization of a long-chain acyl-coenzyme A synthetase encoding gene from the marine microalga *Nannochloropsis oculata*. *Journal of Applied Phycology* **24**: 873-880.

Zhang R, Patena W, Armbruster U, Gang SS, Blum SR, Jonikas MC. 2014. High-throughput genotyping of green algal mutants reveals random distribution of mutagenic insertion sites and endonucleolytic cleavage of transforming DNA. *The Plant Cell* **26**: 1398–1409.

Zhang Y, Ye Y, Bai F, Liu J. 2021. The oleaginous astaxanthin-producing alga *Chromochloris zofingiensis*: potential from production to an emerging model for studying lipid metabolism and carotenogenesis. *Biotechnology for Biofuels* **14**: 119.

Zhao H, Kosma DK, Lü S. 2021. Functional role of long-chain acyl-CoA synthetases in plant development and stress responses. *Frontiers in Plant Science* **12**: 640996-640996.

Zhao L, Haslam TM, Sonntag A, Molina I, Kunst L. 2019. Functional overlap of long-chain acyl-CoA synthetases in Arabidopsis. *Plant and Cell Physiology* **60**: 1041-1054.

Zhao L, Katavic V, Li F, Haughn GW, Kunst L. 2010. Insertional mutant analysis reveals that long-chain acyl-CoA synthetase 1 (LACS1), but not LACS8, functionally overlaps with LACS9 in Arabidopsis seed oil biosynthesis. *The Plant Journal* **64**: 1048-1058.

Zou Z, Tong F, Færgeman NJ, Borsting C, Black PN, DiRusso CC. 2003. Vectorial acylation in *Saccharomyces cerevisiae*: Fat1p and fatty acyl-CoA synthetase are interacting components of a fatty acid import complex. *Journal of Biological Chemistry* **278**: 16414-16422.

Figure legends

Fig. 1 Growth, lipid levels and transcriptional expression of *CrLACS* genes in Chlamydomonas under various N status.

(a) Schematic illustration of three-stage culture conditions (sequentially N replete - NR, N deprivation - ND, then N deprivation-then-recovery - NDR). (b) Cell numbers. (c) TFA and TAG contents. (d) Transcript levels of *CrLACS1*, *CrLACS2* and *CrLACS3* relative to the internal control gene *β-actin*, quantified by RT-qPCR. MM, minimal medium without acetate. Data represent mean ± SD (*n*=3).

Fig. 2 Functional characterization of CrLACS1, CrLACS2 and CrLACS3.

(a) Growth of YB525 cells carrying the empty vector pYES2 or *CrLACS* genes fed on various free fatty acids (FFAs). Yeast growth was recorded at OD 600 nm after 10 days of cultivation. (b) SDS-PAGE separation of recombinant CrLACS1, CrLACS2 and CrLACS3 proteins from *E. coli*. (c) *In vitro* enzymatic assay of CrLACS proteins on various FFAs. Data in (a, c) represent mean ± SD (*n*=3).

Fig. 3 Molecular characterization of the insertional mutants *crlacs1-1* and *crlacs3-1*.

(a, b) Schematic map (a) and PCR validation (b) of the insertion site in *CrLACS1* for *crlacs1-1*. (c) Transcriptional levels of *CrLACS1* in *crlacs1-1* relative to WT. (d, e) Schematic map (d) and PCR validation (e) of the insertion site in *CrLACS3* for *crlacs3-1*. (f) Transcriptional levels of *CrLACS3* in *crlacs3-1* relative to WT. Arrows in (a, d) designate primers used for validating insertion of the cassette. Data in (c, f) represent mean ± SD (*n*=3).

Fig. 4 Comparison of growth and lipids between WT and *crlacs1-1* cells under NR, ND and NDR conditions.

(a) Cell number per mL. (b) TFA content. (c) TAG content. (d) Fluorescent microscopy observation of Bodipy-stained algal cells (ND day 3). Green signals indicate lipid droplets. (e) Percentage of remaining TAG under NDR conditions (relative to ND day

3). Data in (a-c, f) represent mean ± SD (*n*=3). Asterisks indicate the significant difference (Student's *t*-test, *P*<0.05* or *P*<0.01**).

Fig. 5 Comparison of growth and lipids between WT and *crlacs3-1* cells under NR, ND and NDR conditions.

(a) Cell number per mL. (b) TFA content. (c) TAG content. (d) Fluorescent microscopy observation of Bodipy-stained algal cells (day 3 of NDR). Green signals indicate lipid droplets. (e) Percentage of remaining TAG under NDR conditions (relative to ND day 3). Data in (a-c, f) represent mean ± SD (*n*=3). Asterisks indicate the significant difference (Student's *t*-test, *P*<0.05* or *P*<0.01**).

Fig. 6 Contents of membrane lipid classes in WT and mutants under NR and ND conditions.

(a) NR day 3. (b) ND day 3. Data represent mean ± SD (*n*=3). Asterisks indicate the significant difference (Student's *t*-test, *P*<0.05* or *P*<0.01**).

Fig. 7 Complementation of *crlacs1-1* and *crlacs3-1* strains.

(a) The transcript levels of *CrLACS1* (relative to *β-actin*) in WT, *crlacs1-1* and the complemented strains on day 3 of ND as determined by RT-qPCR. (b) TAG contents in WT, *crlacs1-1* and the complemented strains under NR, ND and NDR conditions. (c) Contents of polar lipids in WT, *crlacs1-1* and the complemented strains on day 3 of ND. (d) The transcript levels of *CrLACS3* (relative to *β-actin*) in WT, *crlacs3-1* and the complemented strains on day 3 of NDR as determined by RT-qPCR. (e) TAG contents in WT, *crlacs3-1* and the complemented strains under ND and NDR conditions. (f) Percentage of remaining TAG on day 3 of NDR (relative to ND day 3) in WT, *crlacs3-1* and the complemented strains. Data represent mean ± SD (*n*=3). Different letters above the bars in each group indicate significant difference (p<0.05), based on one-way analysis of variance (ANOVA) and Tukey's honestly significant difference (HSD) test.

Fig. 8 Proposed model explaining that CrLACS1, CrLACS2 and CrLACS3 function spatially and temporally to achieve lipid homeostasis for growth and energy storage in Chlamydomonas.

Multiple organelles are involved in lipid metabolism, including the chloroplast, ER, LDs and peroxisomes, etc. CrLACS1 and CrLACS2 reside in the ER and/or LDs, and contribute to TAG biosynthesis, while CrLACS3 is localized in peroxisomes and contributes to TAG degradation. Under NR condition, growth is active for cell reproduction; acyls are allocated predominantly to chloroplast membrane lipids (CMLs) and ER membrane lipids (EMLs), with a basal level of TAG. Under ND condition, growth is arrested; membrane lipid remodeling and TAG biosynthesis are stimulated while TAG catabolism is minimized, leading to massive accumulation of TAG for energy and carbon storage. Suppression of *CrLACS1* and *CrLACS2* each impairs TAG accumulation with increased levels of CMLs particularly MGDG and DGDG. Exposing ND-treated cells to NDR condition, TAG biosynthesis is minimized while TAG catabolism is stimulated, resulting in TAG degradation to supply carbon and energy sources for cell re-growth. *CrLACS3* suppression severely impairs TAG degradation and thus the cell re-growth. The thickness of green arrows refer to acyl fluxes (not on scale).

Short legends for supporting information

Additional Supporting Information may be found online in the Supporting Information at the end of the article.

Fig. S1 Schematic map for expression of *CrLACS* genes in yeast (a), *E coli* (b) and in Chlamydomonas (c).

Fig. S2 Phylogenetic analysis of Chlamydomonas LACSs and their homologs from other organisms.

Fig. S3 Characterization of the insertional mutant *crlacs1-2*.

Fig. S4 Molecular confirmation of the insertional mutant of *crlacs2-1*.

Fig. S5 Comparison of dry weight per mL and per 10^6 cells between WT and mutants

under ND and NDR conditions.

Fig. S6 Fatty acid composition of TFA and TAG of WT and *crlacs1-1* under NR, ND and NDR conditions.

Fig. S7 Comparison of growth and lipids between WT and *crlacs2-1* cells under NR, ND and NDR conditions.

Fig. S8 Fatty acid composition of TFA and TAG of WT and *crlacs2-1* under NR, ND and NDR conditions.

Fig. S9 Fatty acid composition of TFA and TAG of WT and *crlacs3-1* under NR, ND and NDR conditions.

Fig. S10 Global analysis of RNA-seq samples.

Fig. S11 Transcriptional expression of *CrLACS2* and *CrLACS3* in *crlacs1-1* (up) and of *CrLACS1* and *CrLACS3* in *crlacs2-1* (down) under NR and ND conditions.

Fig. S12 Heterologous expression of *CrLACS* genes in yeast promoted lipid synthesis.

Table S1 Primers used in the present study.

Table S2 Features of *CrLACS* genes.

Data S1 FPKM values of all samples.

Data S2 The RNA-Seq data for genes involved in selected biological pathways.